Relationship among MJO, westerly wind bursts, tropical cyclones and mid-latitude baroclinic waves observed in an idealistic aqua-planet NICAM simulation

YOSHIZAKI Masanori* WATARAI Yasushi*
SUZUKI-PARKER Asuka* MORIIZUMI Shin-ichi**

Key words：NICAM, MJO, westerly wind burst, tropical cyclone, mid-latitude baroclinic wave

1. Introduction;

In tropics, convective activity of cumulonimbi is active, and disturbances with various horizontal scales and propagating speeds are seen due to diabatic heating of cloud clusters. Hereafter, disturbances with a horizontal scale greater than 1000 km are focused on. Madden and Julian (1971) found that cloud disturbances having several 1000 km scales propagate eastward slowly with a speed of about 5 m s^{-1}, forming over the Indian Ocean and decaying over the western Pacific Ocean repeatedly with 30-60 day period (Madden-Julian Oscillation; MJO). By analyzing equatorial disturbances using satellite data, Wheeler and Kiladis (1999) showed MJO, fast eastward-propagating disturbances with speeds of 15-25 m s^{-1} and slow westward-propagating disturbances as symmetric equatorial mode, as well as mixed Rossby-gravity wave-like disturbances as anti-symmetric equatorial one. These disturbances have considerably slow propagating speeds compared with those in the dry atmosphere, indicating that they might be related to moist properties. In the off-equatorial region from the latitude 5 degrees, tropical cyclones (TCs) frequently emerge due to diabatic heating of cloud clusters and some TCs develop into typhoons which have wind speeds greater than, for example, 17 m s^{-1} in the north-eastern Pacific Ocean.

Over the equatorial troposphere, easterly winds generally prevail in the lower troposphere, since the Hadley circulation is dominant. However, westerly winds are generated due to intense convective activity of cloud clusters, and intense westerly winds are called as westerly wind bursts (WWBs). The Rossby response of diabatic heating might be a candidate for the formation of westerly winds (Gill 1980). However, WWBs are also generated in other situations and, thus, atmospheric motions are complicated.

Historically speaking, CISK (conditional instability of the second kind) (Charney and Eliassen, 1964) mechanism was the first proposed mechanism for genesis and development of TCs. Over the western North Pacific, a number of studies examined the large-scale environmental factors contributing to TC genesis (Briegel and Frank, 1997, Ritchie and Holland, 1999, Yoshida and Ishikawa, 2013, Fudeyasu and Yoshida, 2018, Fudeyasu et al., 2019). Yoshida and Ishikawa (2013) categorized TC genesis into five flow patterns: shear line, confluence region, gyre, easterly wave and preexisting TC, and showed that the most favorable case is shear line accounting for 42 percent. Other studies examined TC genesis process at meso-scale. Proposed mechanisms can be categorized to top-down and bottom-up one. In the top-down assumption, several vortices in the stratiform clouds of cloud clusters enhance from middle to lower levels, and develop into a TC (Ritchie and Holland 1997, Simpson et al. 1997, Bister and Emanuel 1997). In the bottom-up assumption, on the other hand, several intense vortices in the lower level associated with cumulonimbus clouds

* Faculty of Geo-Environmental Science, Rissho University
** Graduate School of Geo-Environmental Science, Rissho University

merge and develop into a TC（Hendricks et al. 2004, Montgomery et al. 2006）.

Recently, global cloud-resolving models developed with improvement of the super-computer and so on, and one model is a NICAM（Satoh, 2003）, which is an abbreviation of Nonhydrostatic ICosahedral Atmospheric Model. This model contains full atmospheric dynamics and physical processes, including radiation, cloud microphysics, and boundary-layer processes. In particular, the cloud microphysics process solves water vapor, cloud water, cloud ice, rain, snow, and graupel as prognostic variables, and the NICAM can represent temporal variations and structures of cumulonimbus clouds and cloud clusters. Nasuno et al.（2007, 2008）simulated fast eastward-propagating disturbances with a speed of about 17 m s^{-1}（called as super cloud clusters, SCCs）and westward-propagating ones on the idealistic sea surface temperature（SST）aqua-planet, forcing the Hadley circulation in the latitudinal direction. An aqua-planet simulation assumes the earth covered by water with no land. The model atmosphere is forced by idealistic, time-invariant SST. Using such models, it is anticipated that simple atmospheric motions can be reproduced, since complicated real land and sea distribution, complex uneven terrains and nonlinear interaction between ocean and atmosphere are removed. Then, these outputs are beneficial for deep understandings, for example, about formation and development of disturbances.

In this study, analyses are made using the NICAM aqua-planet outputs under an idealized SST distribution. The SST forcing is such that it induces Hadley and Walker circulations in latitudinal and longitudinal directions, respectively. Since MJO-like disturbances and TCs are well simulated, relationships among MJOs, WWBs, TCs, and mid-latitude baroclinic waves are examined, focusing on the formation of TCs.

2. Descriptions of an idealistic aqua-planet NICAM simulation:

(a) Descriptions of SST forcing:

Figure 1a shows the distribution of idealized, time-invariant SST forcing given in the aqua-planet NICAM simulation（Iga et al. 2010）. SST is the maximum at the equatorial central area（latitude = 0 degree, and longitude = 0 degree）, and falls in both latitudinal and longitudinal directions. Fig. 1b shows a meridional cross-section of SST forcing at the longitude 0 degree. Since the SST is symmetric about the equator, upward motions are excited in tropics and the Hadley circulation develops there. In the range between about 10 and 60 degrees in the latitudinal direction in both hemispheres, the SST gradient is large and baroclinic unstable waves appear there. In higher latitudes greater than 60 degrees, the SST is nearly constant and no disturbance is forced there. Fig. 1c shows a longitudinal cross-section of SST forcing at the latitude 0 degree. In longitudinal direction, SST is spatially varied to follow a sinusoidal curve, with wavenumber 1 and the amplitude of 4.5 K（ΔT=4.5）. This SST variation in the longitudinal direction produces the Walker circulation. An area denoted by a thick red line（90 W-90 E）is hereafter referred to as the high SST area.

(b) Data for analysis:

The NICAM simulation was conducted for the total of 240 days. Analysis was performed for the last 180 days of simulation, with the first 60 days discarded as the model spin-up time. An original data for analysis are 2560 × 1280 horizontal grids（14 km horizontal resolution）and 54 layers in the vertical direction, and rearranged into two data sets. The first dataset is 860 × 400 horizontal grids（14 km horizontal resolution）（a rectangle denoted by red broken-lines in Fig. 1a）and 45 layers in the vertical direction, where the upper levels are cut off. The second dataset is 360 × 180 horizontal grids（averaged about 100 km horizontal resolution from the original data）and 54 layers in the vertical direction. These datasets have time-series data for 3 hour interval about 3 dimensional variables, such as zonal velocity, u; meridional velocity, v; vertical velocity, w; potential temperature, θ ; diabatic heating, dh; and vertical vorticity, ς ; and for one hour interval about 2 dimensional variables, such as precipitation; and outgoing longwave radiation, OLR.

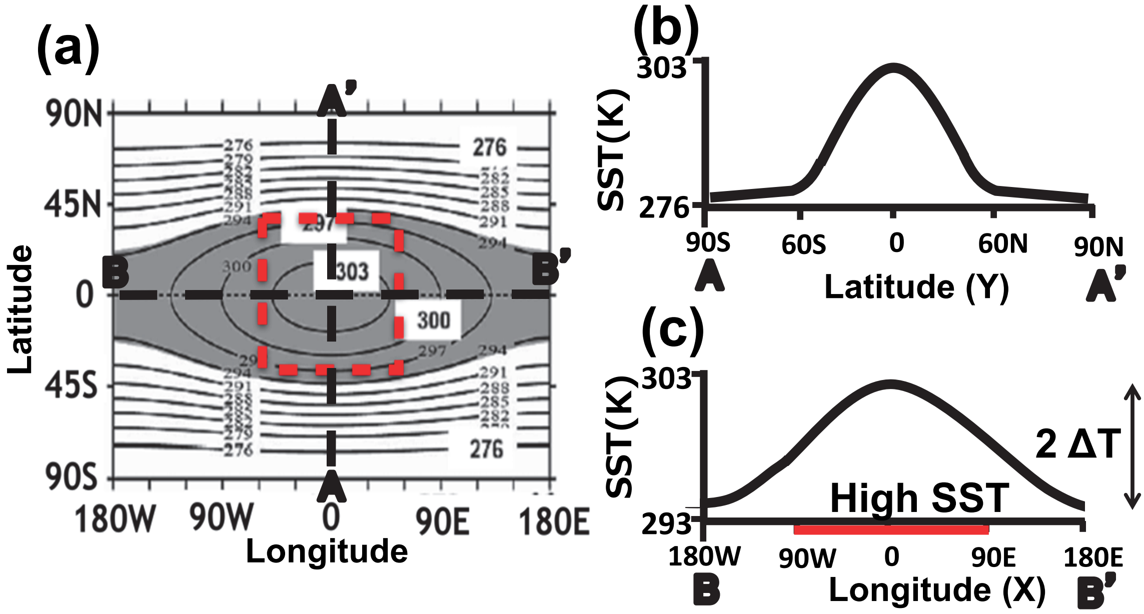

Fig.1: (a) Horizontal distribution of SST (Iga et al. 2010), (b) meridional section at the longitude 0 degree, and (c) longitudinal section at the latitude 0 degree, where wavenumber 1 and amplitude of 4.5 K (ΔT=4.5) are forced. A rectangle denoted by red broken-lines in (a) is a horizontal area where the grid resolution is 14 km. An area denoted by a thick red line between 90 W and 90 E in (c) is a high SST one.

(c) Classification of propagating disturbances and vortexes:

As shown later in the Section 3, the NICAM simulation produced large-scale disturbances accompanied with diabatic heating in tropics, in particular, over the high SST area. Since large-scale disturbances have top-heavy heating profiles in the vertical direction, they generally have a propagation property, and, in particular, eastward-propagating disturbances are likely to appear on the equatorial beta plane (Yoshizaki, 1991a, 1991b). Propagating speeds of these disturbances in the NICAM simulation are determined at a 10 m s^{-1} interval. For example, disturbances with propagation speeds of 10-20 m s^{-1} are denoted as ones having propagation speeds of 15 m s^{-1}.

Cyclonic vortexes are divided into three types according to their maximum wind speeds at the height of 807 m (model level); weak cyclonic vortexes, TCs, and typhoons. Consider Rankine's vortexes with maximum wind speed at the 50 km distant from the vortex center. The vortexes with maximum wind speeds of 7.5 m s^{-1} or less are categorized as weak cyclonic vortexes, ones with maximum wind speeds greater than 7.5 m s^{-1} or less than 15 m s^{-1} are categorized as TCs, and ones with maximum wind speeds exceeding 15 m s^{-1} are categorized as typhoons. For example, the TC can be represented as the vorticity painted by a yellow-color in Fig. 5e.

3. Results:

(a) Classification of disturbances in tropics:

Figure 2 shows a longitude-time cross section of precipitation over tropics. In whole areas, both eastward- and westward-propagating disturbances are seen. Focusing on high SST areas, eastward-propagating disturbances appear mostly, and, in particular, intense precipitation areas are found in the range from about 60 W to 5 W. Here, disturbances propagate eastward slowly with a speed of about 5 m s^{-1}. On the low SST areas, on the other hand, precipitation intensity is weak and most disturbances propagate westward with a speed of about -15 m s^{-1}.

Figure 3 is a longitude-time cross section of u at the height of 807 m over tropics. In the range from about 120 W to 30 E, westerly winds are seen, while easterly

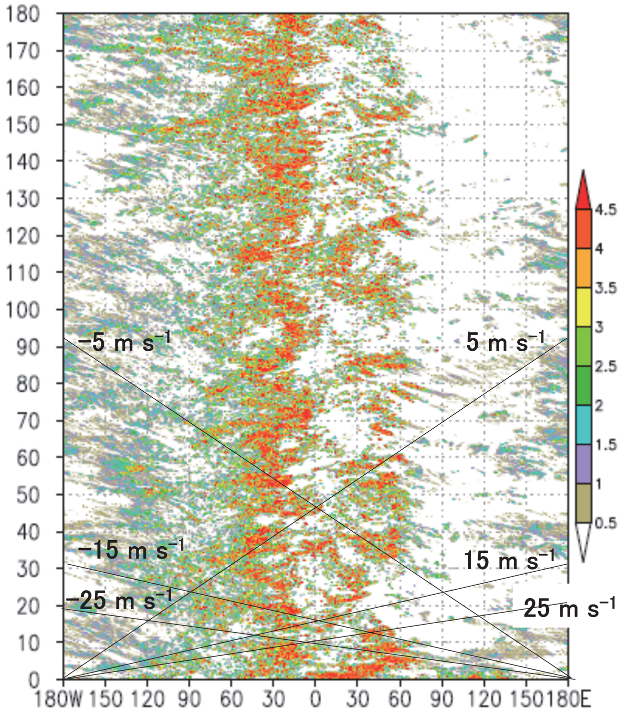

Fig.2: Longitude-time cross section of precipitation (mm h^{-1}) averaged between 3 S to 3 N in the latitudinal direction. Solid lines denote propagation speeds of disturbances, where a positive (negative) value means eastward (westward) propagation.

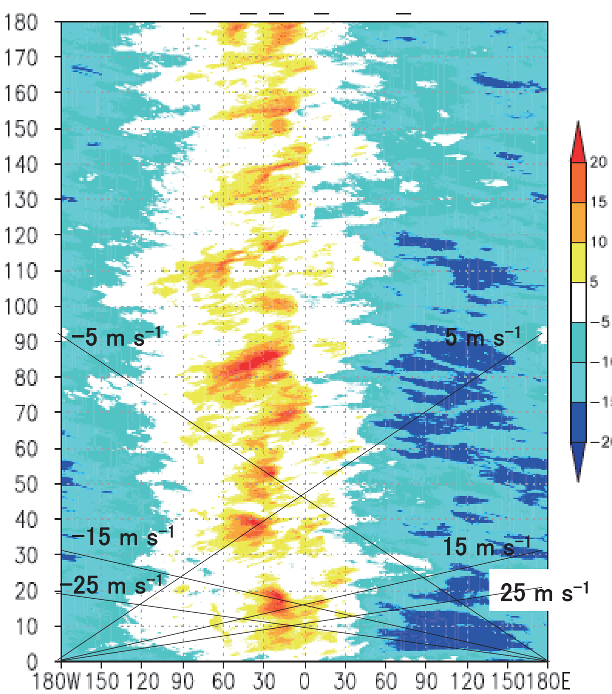

Fig.3: Longitude-time cross section of zonal wind u (m s^{-1}) at the height of 807 m averaged between 3 S to 3 N in the latitudinal direction. Solid lines denote propagation speeds of disturbances, where a positive (negative) value means eastward (westward) propagation.

winds are dominant in other areas. Westerly winds are found in the intense diabatic heating on the high SST areas, and, in particular, intense westerly winds are generated in a range from about 60 W to 30 W. Hereafter, WWBs are defined as westerly wind with an intensity greater than 10 m s^{-1}.

Figure 4 shows a longitude-time cross section of OLR smaller than 220 W m^{-2} and WWB areas over tropics. As Fig.2, eastward-propagating disturbances are remarkable in the smaller OLR areas and representative eastward-propagating ones are denoted as system A to system J (black dotted lines). These systems have a life cycle to form, develop, and decay repeatedly with periods of 15-30 days. Since these systems have a common propagation speed and a life cycle similar to MJO observed in tropics, they are called “MJO-like disturbances”. Some MJO-like disturbances are related to WWBs, but not always. One example is shown in a black elliptic line in Fig. 4.

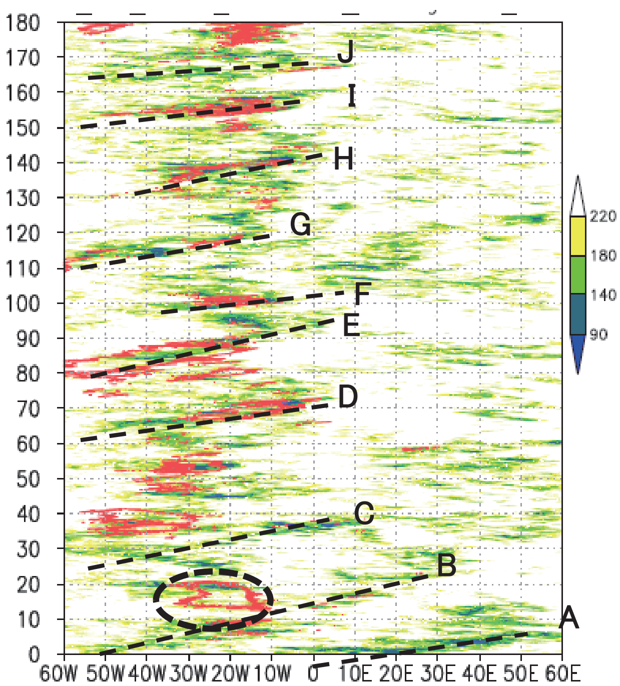

Fig.4: Longitude-time cross section of OLR (W m^{-2}) averaged between 3 S to 3 N in the latitudinal direction and WWB areas encircled by red lines. Broken lines denoted by alphabets indicate propagation speeds of disturbances, where a positive (negative) value means eastward (westward) propagation. Note that the interval of longitude is different from those in Figs. 2 and 3.

Upper figures in Fig. 5 show time-series of longitude-vertical cross sections of dh, θ, and wind vectors (u, w) at the equator at 9 h in 5, 8, 11, 14, 17 and 20 day. An MJO-like disturbance denoted by red elliptic lines is traced, where high dh areas propagate eastward with high cloud-top reaching about 16 km in Figs. 5a, 5b, 5c and 5d. Lower figures of Fig. 5 show horizontal distributions of ς and θ, at the height of 5640 m and wind vectors (u, v) at the height of 807 m. The MJO-like disturbance induces intense westerly winds over tropics (Fig. 5b), inducing the WWB as a Rossby response of heating in off-equatorial areas on its western side (Figs. 5c, 5d). However, other WWBs are similarly excited around TCs where twin cyclones are found on both hemispheres (Fig. 5e). The WWB denoted by a black elliptic broken-line in Fig. 5e corresponds to one in Fig. 4. In this way, WWBs are induced by, at least, two ways: Rossby response of heating and TCs. Therefore, WWBs should not be said as disturbances, which induce intense westerly winds, but they rather are produced by disturbances such as MJO-like ones or TCs.

(b) Relationship between WWBs and mid-latitude baroclinic waves, and formation of TCs:

10 several TCs are seen in both hemispheres during 180 day simulation. Normally one TC is seen in one hemisphere, while twin cyclones straddling both hemispheres and four TCs occasionally appeared.

Here we focus on the relationship between westerly wind areas in the tropics, and anticyclonic circulation associated with mid-latitude baroclinic waves. In the lower figures of Fig. 5, the WWB is indicated by red solid arrows, and the anticyclonic circulation is indicated by dashed arc-shaped arrows. The center of anticyclonic circulation is denoted by H. Mid-latitude baroclinic waves with large scales of about 5000 km repeatedly move eastward on both hemispheres between 30-40 latitude degrees. The amplitude of mid-latitude baroclinic waves intensifies to produce anticyclonic circulation around 10-30 latitude degrees. Along with the WWB, the easterly winds on the equator-sides of the anticyclonic circulation induces strong horizontal wind shear in the meridional direction. This horizontal wind shear helps to produce cyclonic vortexes with sizes of several 100 km shown by circles. In Fig. 5b, a weak cyclonic vortex is found around the area (~15 W, ~5 S), slowly moving southward, and develops into a TC in Fig. 5e. In the northern hemisphere, a weak cyclonic vortex in Fig. 5d is seen around the area (~15 W, ~5 N) first, and develops into a TC, similarly to the southern hemisphere case. In both cases, intense horizontal wind shear is found where weak cyclonic vortexes develop.

Figure 6 shows a longitude-time cross section of TC formation and anticyclonic circulations associated with mid-latitude baroclinic waves. During 180 day simulation, it is summarized that anticyclonic circulations preceded the formation of TCs in most cases. However, the places of the TC formation are not always fixed relatively to anticyclonic circulations.

4. Discussions:

(a) Comparison of ΔT=4.5 case with ΔT=0 and ΔT=2.25 cases:

In Yoshizaki et al. (2012), the impact of SST was studied by changing the longitudinal variations of SST with ΔT=0, 2.25, and 4.5. In the ΔT=0 case (in which SST is uniform in the longitudinal direction), fast eastward-propagating SCCs with a speed of about 15 m s^{-1} are dominant in tropics, whereas fast westward-propagating ones are also found. In the ΔT=2.25 case, some differences are seen between high and low SST areas. On the contrary, in the ΔT=4.5 case, slow eastward-propagating disturbances with a speed of about 5 m s^{-1} (MJO-like disturbances) appear, and no fast eastward-propagating one like SCC appear. In addition, 10 several TCs are generated in both hemispheres during 180 day simulation.

The SST variation of ΔT=4.5 used in this study seems large compared with the SST observed in the maritime continent (Indonesia area) and the eastern Pacific Ocean. In this study, an atmospheric general circulation is induced only by this SST variation. Comparing our study with realistic situation, thermal and dynamic forcing such as land-sea contract and topography should be added as forcing to atmospheric

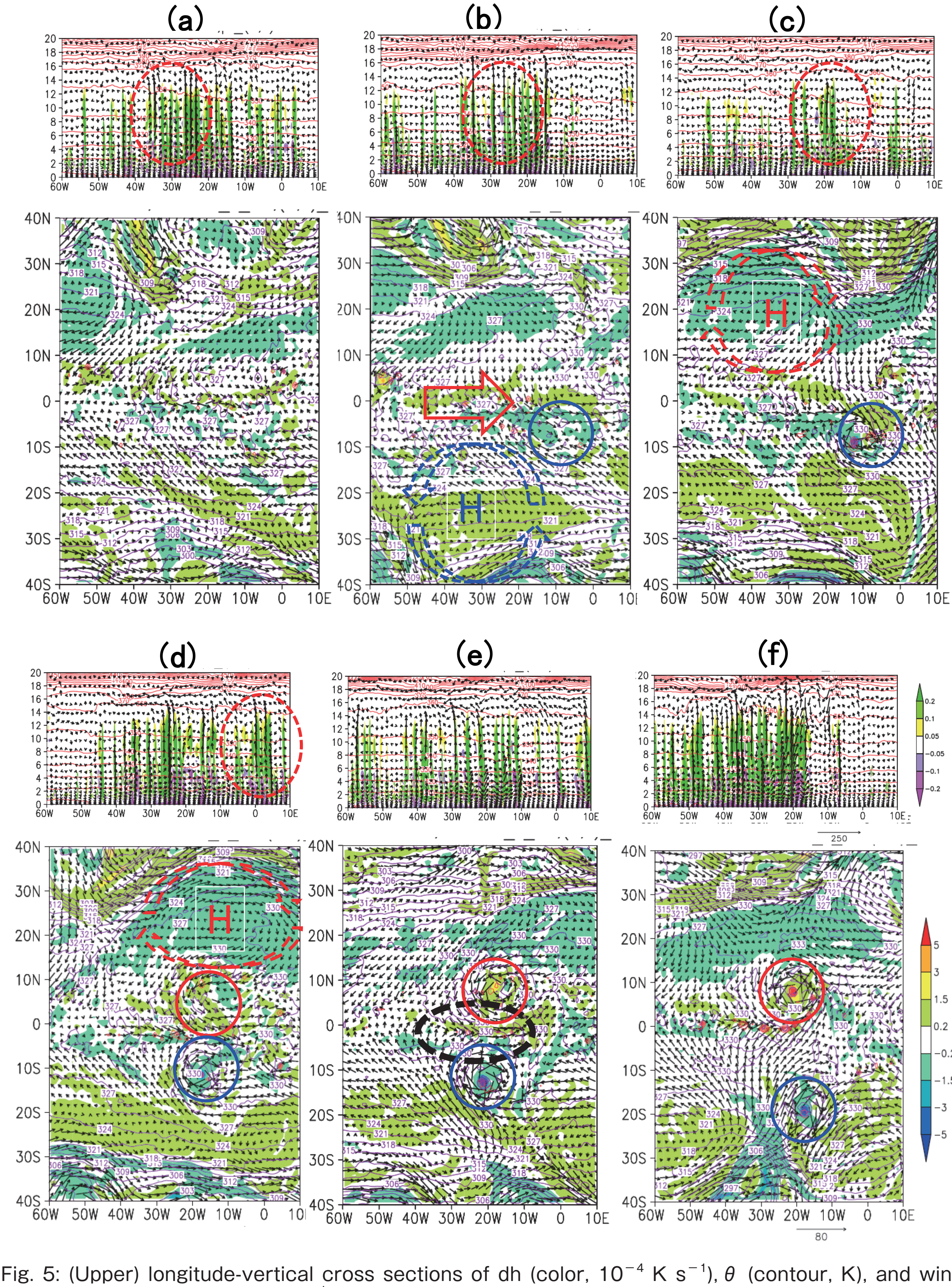

Fig. 5: (Upper) longitude-vertical cross sections of dh (color, 10^{-4} K s^{-1}), θ (contour, K), and wind vectors (u, w) (arrows, m s^{-1}) at the equator at 9 h in (a) 5, (b) 8, (c) 11, (d) 14, (e) 17 and (f) 20 day, and (lower) horizontal distributions of ς (color, 10^{-4} s^{-1}) and θ (contour, K) at the height of 5640 m, and wind vectors (u, v) (arrows, m s^{-1}) at the height of 807 m. In the upper figures, dashed red ovals mean areas shown in the line B in Fig. 4. In the lower figures, large-scale anticyclonic circulations and vortexes are shown by dashed arc-shaped arrows and circles, respectively. The centers of anticyclonic circulation are denoted by H.

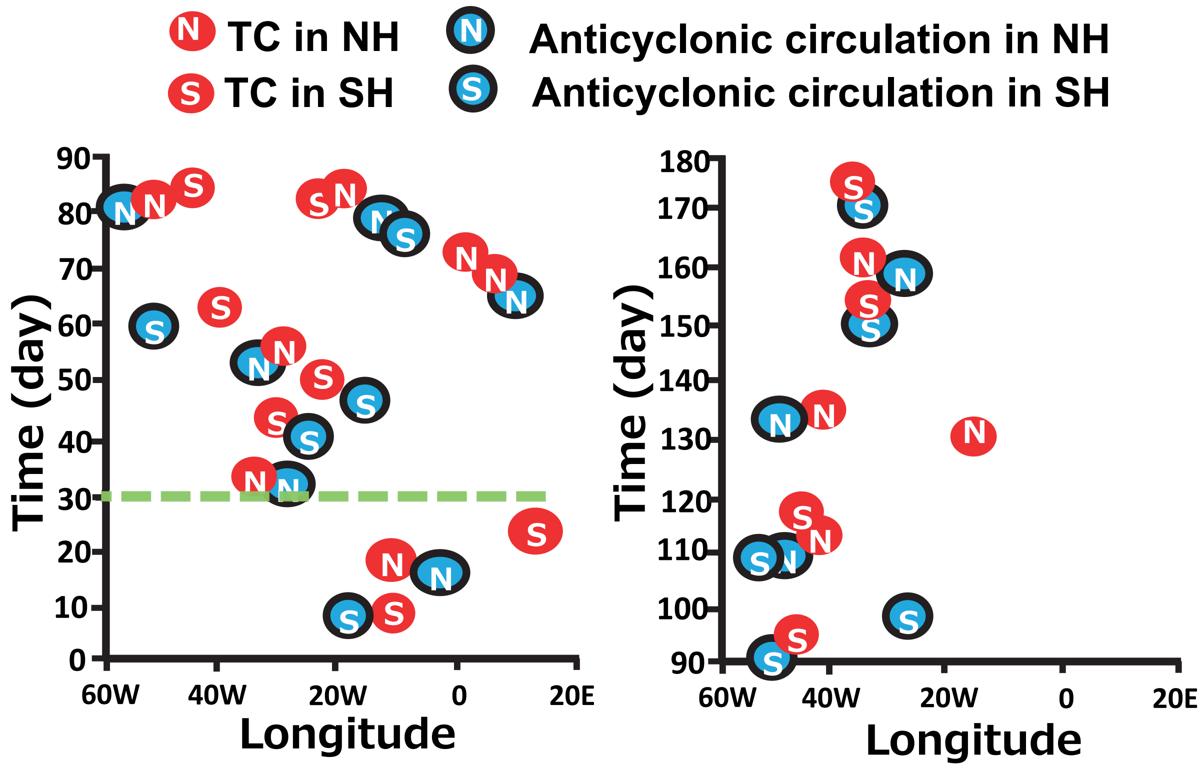

Fig.6: Longitude-time cross section of TC formations and anticyclonic circulation of mid-latitude baroclinic waves.

motion in the realistic situation. Similarly, by changing the topography of the maritime continent using the NICAM with a 220-km horizontal mesh, Takasuka et al. (2015) showed that the zonal contrast of latent heat flux enhances eastward propagation of MJO-like disturbance. Thus, the $\Delta T=4.5$ is not too large when real dynamic and thermal forcing is considered.

(b) Application of TC formation to realistic situation:

Based on the idealistic aqua-planet NICAM simulation, this study demonstrated that TCs often formed when eastward-propagating anticyclonic circulation associated with mid-latitude baroclinic waves approached the WWBs at appropriate timings. However, such situations do not frequently occur in the real warm period over the Pacific Ocean. Preferable areas for the TC formation in the real situation are the northwestern Pacific Ocean where the monsoon trough is frequently observed on the eastern part of Indonesia under the planetary-scale Pacific-scale sub-high zone. In most cases, the interaction between WWBs and monsoon trough produces the horizontal shear instability, resulting in the formation of cyclonic vortexes and TCs.

5. Summary:

Analyses were conducted using an aqua-planet NICAM simulation with idealized SST forcing. The SST forcing is such that it induces Hadley and Walker circulations in latitudinal and longitudinal directions, respectively. In tropics, MJO-like disturbances, WWBs and TCs frequently appeared. WWBs appeared in several ways, such as (1) the Rossby response of diabatic heating from MJO-like disturbances and others, and (2) developing TCs. The relationship of WWBs and anticyclonic circulations associated with mid-latitude baroclinic waves was studied for the formation of cyclonic vortexes. It is found that in most cases anticyclonic circulations associated with mid-latitude baroclinic waves first approached WWBs and then intensified cyclonic vortexes, sometimes developing into TCs. However, the interaction of mid-latitude baroclinic waves and WWBs rarely occurs in real situation. This interaction is considered to appear as the monsoon trough accompanied with sub-high zone over the Pacific Ocean, with horizontal scales of about 10,000 km. The monsoon trough may work to induce horizontal shear and help weak cyclonic vortexes to develop into TCs.

Acknowledgement:

The authors thank reviewers for improving the draft, and Prof. M. Satoh（Atmosphere and Ocean Research Institute, Univ. Tokyo）and Dr. S. Iga（Research Organization for Information Science and Technology）for providing the NICAM data.

References:

Bister, M. and K. A. Emanuel, 1997: The genesis of Hurricane Guillermo: TEXMEX analyses and a modeling study. *Mon. Wea. Res*., **125**, 2662-2682.

Briegel, L. M. and W. M. Frank, 1997: Large-scale influences on tropical cyclogenesis in the western north Pacific. *Mon. Wea. Res*., **125**, 1397-1413.

Charney, J. G. and A. Eliassen, 1964: On the growth of the hurricane depression. *J. Atmos. Sci.*, **21**, 68-75.

Emanuel, K. A., 1986: An air-sea interaction theory for tropical cyclones. Part I: Steady-state maintenance. *J. Atmos. Sci*., **43**, 585-604.

Fudeyasu, H. and R. Yoshida 2018: Western North Pacific tropical cyclone characteristics stratified by genesis environment, *Mon. Wea. Rev*., **146**, 435-446.

Fudeyasu, H., R. Yoshida, M. Yamaguchi, H. Eito, C. Muroi, S. Nishimura, K. Bessho, Y. Oikawa, and N, Koide, 2019: Development conditions for tropical storms over the western North Pacific stratified by large-scale flow patterns. *J. Meteor. Soc. Japan*, Early Online Release. https://www.jstage.jst.go.jp/article/jmsj/advpub/0/advpub_2020-004/_article/-char/ja/

Gill, A. E. 1980: Some simple solutions for heat-induced tropical circulation. *Quart. J. Roy. Met. Soc.*, **106**, 447-462.

Hendricks, E. A., M. T. Montgomery, and C. A. Davis, 2004: The role of "vortical" hot towers in the formation of tropical cyclone Diana（1984）. *J. Atmos. Sci*., **61**, 1209-1232.

Iga, S., M. Yoshizaki, M. Satoh, T. Nasuno, H. Tomita, and K. Yasunaga, 2010: Global aquaplanet experiments using the NICAM new codes（in Japanese）. *Proc. Spring Meeting, Japan Meteor. Soc*., **97**, 76.

Love, G, 1985: Cross-equatorial influence of winter hemisphere subtropical cold surges. *Mon. Wea. Res*., **113**, 1487-1498.

Madden. R. A. and P. R. Julian, 1971: Detection of a 40-50 day oscillation in the zonal wind in the tropical Pacific. *J. Atmos. Sci*., **28**, 702-708.

Montgomery, M. T., M. E. Nicholls, T. A. Cram and A. B. Saunders, 2006: A vortical hot tower route to tropical cyclogenesis. *J. Atmos. Sci*., **63**, 355-386.

Nasuno, T., H. Tomita, S. Iga, H. Miura, and M. Satoh, 2007: Multiscale organization of convection simulated with explicit cloud processes on an aquaplanet. *J. Atmos. Sci*., **64**, 1902-1921.

Nasuno, T., H. Tomita, S. Iga, H. Miura, and M. Satoh, 2008: Convectively coupled equatorial waves simulated on an aquaplanet in a global nonhydrostatic experiment. *J. Atmos. Sci*., **65**, 1246-1265.

Ritchie, E. A., and G. J. Holland, 1997: Scale interactions during the formation of typhoon Irving. *Mon. Wea. Res*., **125**, 1377-1396.

Ritchie, E. A., and G. J. Holland, 1999: Large-scale patterns associated with tropical cyclogenesis in the western Pacific. *Mon. Wea. Rev*., **127**, 2027-2043.

Satoh, M., 2003: Conservative scheme for a compressible nonhydrostatic model with moist processes. *Mon. Wea. Rev*., **131**, 1033-1050.

Simpson, J. E., E. A. Ritchie, G. J. Holland, J. Halverson and S. Stewart, 1997: Mesoscale interactions in tropical cyclone genesis. *Mon. Wea. Res*., **125**, 2643-2661.

Takasuka, D., T. Miyakawa, M. Satoh, and H. Miura, 2015, Topographical effects on internally produced MJO-like disturbances in an aqua-planet version of NICAM. *SOLA,* **11**, 170-176.

Wheeler, M. and G. N. Kiladis, 1999: Convectively coupled equatorial waves: Analysis of clouds and temperature in the wavenumber-frequency domain. *J. Atmos. Sci*., **56**, 374-399.

Yoshida, R. and H. Ishikawa, 2013: Environmental factors contributing to tropical cyclone genesis over the western North Pacific. *Mon. Wea. Res*., **141**, 451-467.

Yoshizaki, M., 1991a: Selective amplification of the eastward-propagating mode in a positive-only wave-CISK model on an equatorial beta plane. *J. Meteor. Soc. Japan*, **69**, 353-373.

Yoshizaki, M., 1991b: On the selection of eastward-propagating mode appearing in the wave-CISK model as tropical intraseasonal（30-60-day）oscillations -linear responses to localized heating moving in the east-west direction on the equatorial beta plane-. *J. Meteor. Soc. Japan*, **69**, 595-608.

Yoshizaki, M., K. Yasunaga, S. Iga, M. Satoh, T. Nasuno, A. T. Noda, and H. Tomita, 2012: Why do super clusters and Madden Julian Oscillation exist over the equatorial region? *SOLA*, **8**, 33-36.

理想化された海面水温分布の強制のもとでNICAMの水惑星数値実験に見られたMJO、西風バースト、熱帯低気圧、傾圧不安定波の相互関係

吉 﨑 正 憲* 渡 来 靖* 鈴木パーカー 明日香* 森 泉 慎 一**

*立正大学地球環境科学部
**立正大学大学院地球環境科学研究科

Abstract:

理想化された水温分布の強制のもとでNICAMによる数値実験の結果を用いて、解析を行った。南北にハドレー循環、東西にウォーカー循環を強制するように、水温分布を与えた。熱帯域ではマッデン・ジュリアン振動（MJO）のような東進するじょう乱が見られ、熱帯低気圧（TC）もしばしば発生した。そこでは、少なくとも二つの方法（熱源によるロスビー応答とTC）によって強い西風域（西風バースト：WWB）が形成された。また、TC発生に関してWWBと中緯度帯に現れる傾圧不安定波による高気圧性循環との関係を調べた。その結果、多くの場合、まず高気圧性循環がWWBに近づいて、それから弱い低気圧性の渦が現れ、中にはTCまで発達することが分かった。ここで与えた東西方向のSSTの大きさや中緯度帯の傾圧不安定波が果たしてTCを形成するのかについて議論した。

キーワード：NICAM, マッデン・ジュリアン振動、西風バースト、熱帯低気圧、傾圧不安定波